

# Solar system science with subarcsecond slit spectroscopy

R. Dekany<sup>a</sup>, D. Banfield<sup>b</sup>, M. Brown<sup>c</sup>, A. Bouchez<sup>c</sup>, T. Hayward<sup>b,\*</sup>, B. Brandl<sup>b</sup>,  
B.R. Oppenheimer<sup>c,\*\*</sup>, M. Troy<sup>a</sup>, G. Brack<sup>a</sup>, T. Trinh<sup>a</sup>, F. Shi<sup>a</sup>

<sup>a</sup>Jet Propulsion Laboratory, California Institute of Technology, Pasadena, CA 91109

<sup>b</sup>Cornell University, Ithaca, NY 14853

<sup>c</sup>California Institute of Technology, Pasadena, CA 91125

## Abstract

During its first year of shared-risk observations, the PALAO/PHARO adaptive optics system has been employed to obtain near-infrared  $R \sim 1000$  spectra of solar system targets at spectroscopic slit widths of 0.5 and 0.1 arcsec, and corresponding spatial resolution along the slit as fine as 0.08 arcsec. Phenomena undergoing initial investigation include condensate formation in the atmosphere of Neptune. We present the results of this AO spectroscopy campaign and discuss AO specific considerations in the reduction and interpretation of this data.

**Keywords:** Adaptive optics, slit spectroscopy, Neptune

## Introduction

The Cornell PHARO near-infrared science camera<sup>1</sup>, used in conjunction with the JPL PALAO adaptive optics system at Palomar Mountain, supported the 'shared-risk' science observations for 9 observing programs during the past year. The majority of these programs, approximately 67%, included the collection of  $R \sim 1000$  infrared spectra using the grism spectrometer mode provided by PHARO. Early science results of several of these observations are now in preparation. We choose here to consider one particular subset of observation, namely narrow-slit spectroscopy of solar system objects, and point out both the benefits of adaptive optics for these science programs and the special concerns in the planning, acquisition, and analysis of high-spatial-resolution slit spectra.

## Neptune

Spectroscopic observations of Neptune were obtained during the nights of Aug 26–29, 1999, with PHARO's spectroscopic slit aligned to yield various longitudinal cuts across the disk of the planet. Neptune itself was used as the guide object for the PALAO wavefront sensor. The finite size of the disk ( $\sim 2.5$  arcsec XXX in diameter) did not seem to substantially degrade the PALAO performance, once suitable calibration of the wavefront sensor background level was performed. An example of the spectra obtained is shown in Figure XXX. Between observations of Neptune, spectroscopic calibration data of the star HD190821 were obtained. While data analysis continues, we describe herein our approach to determining AO-enabled atmospheric science of Neptune.

The PHARO camera / spectrograph allows a spectral resolution of about 1000 in the K-band, within which Neptune's atmosphere has pressure-induced molecular hydrogen and strong rotation-vibration methane absorptions. By measuring the reflectivity of the planet across these molecular absorption bands, we can retrieve the vertical distribution of the scatterers reflecting the sunlight as a function of latitude for each of the longitudinal cuts obtained.

Because methane condenses in the tropospheres of Neptune, its abundance as a function of altitude and position is not well known. Indeed, it is very likely dynamically controlled in the troposphere, and hence an interesting quantity to study. The hydrogen abundance is relatively well known, and its S(1) absorption feature around  $2.11 \mu\text{m}$  can then be used to constrain the vertical sampling of the spectra. Using the hydrogen absorption wavelengths, we can retrieve the scatterer vertical distribution from each spectra. Then, methane abundances can be determined by comparing the reflectivities in the hydrogen absorption with those in the methane absorption. Vertical sensitivity extends from the optical depth unity

\* Currently with Gemini Observatory, Hilo, HI 96720

\*\* Currently with University of California, Berkeley, CA 94620

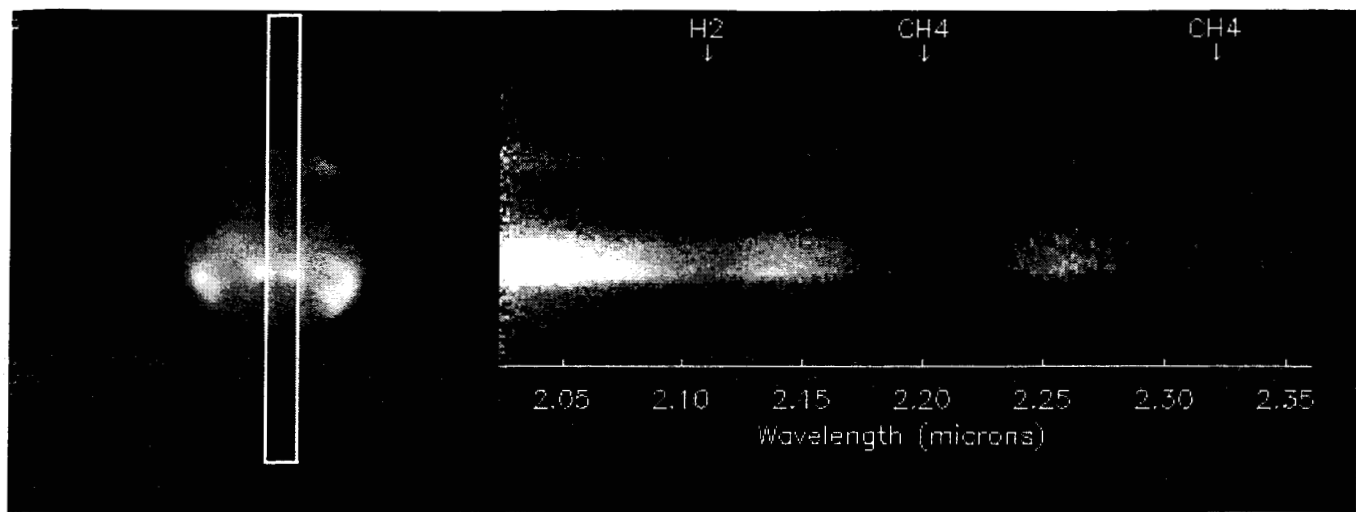


**Figure XXX.** Neptune spectra (right) taken along a longitudinal slice of the AO-corrected disk (left).

level for the most opaque wavelength of hydrogen absorption down to a level where the integrated scatterer optical depth approaches unity. Below this, the single scattering analysis used in our retrieval approach breaks down.

For Neptune, this means pressures of roughly 100 mbar to perhaps 1 bar or more<sup>2</sup>. All of these results will be with significant latitudinal resolution on the planets and (eventually) for multiple longitudinal cuts. With the images already in hand, it is clear that there are discrete cloud features at certain latitudes and longitudes. The results of our detailed analysis when it is completed should clarify many interesting details of the circulation of Neptune's atmosphere.

To absolutely calibrate the spectra, a slightly modified version of the technique used by Banfield, et. al.<sup>3</sup> will be employed. This is to use calibrated narrow band filter images of the planets (calibrated via standard star observations), and then to compare given regions of the planet in these images with corresponding regions within the slit of the spectral images. By constraining the total flux in these regions in the narrow band images to equal that in the spectral images, integrated across the narrow band filter transmission curve, we can absolutely calibrate the spectral images.

For wavelengths at which Neptune has low reflectivity ( $I/F < 0.1$ ), reflected photons will be overwhelmingly only singly scattered. Thus, the relation between scatterer distribution and reflectivity is linear and relatively easy to invert using least squares techniques. This is the approach outlined and used by Banfield, et. al.<sup>2 xxx. 4</sup> to determine Jupiter's scatterer distribution. In those works, we used both hydrogen and methane absorption features to constrain the vertical profile of scatterers, since both gaseous species have well known abundances in the upper troposphere and lower stratosphere of Jupiter. However, for both Neptune, the methane abundance is not likely to be uniform vertically or horizontally because it condenses in the troposphere, nor is it very well known in a disk averaged sense.

We can still employ the known distribution of hydrogen and its known S(1) spectral absorption<sup>5</sup> near 2.11  $\mu\text{m}$  to retrieve the vertical distribution of scatterers for Neptune. This would proceed nearly identically to the previous works for Jupiter, just with a smaller subset of wavelengths. Because the 2.11  $\mu\text{m}$  hydrogen feature is not as opaque as the 2.3  $\mu\text{m}$  methane feature, we will not be able to probe as high in the atmosphere of Neptune. Preliminary estimates of the highest weighting functions due to hydrogen absorption in the K band wavelengths have maxima at around 100 mbar<sup>6</sup>. For the Jupiter work, we were able to sense up to about 20 mbar. The deepest that we can sense is determined by the fact that we can only easily analyze singly scattered photons. By going to the wings of an absorption feature, we can sense deeper and deeper, until the integrated optical depth becomes  $\sim 1$  and reflected photons are likely to be multiply scattered. For Jupiter, this meant that we could sense to about 400 mbar (where the upper tropospheric haze becomes significantly more dense), while for Neptune, we may be able to sense to 1 bar or more<sup>2 xxx. 7</sup>.

We can extend the analysis approach to also yield the methane abundance as a function of altitude much as it yields the scatterer abundance already. Conceptually, the same scatterers which were constrained using the spectra in the hydrogen absorption feature are also causing the reflectivity in the methane absorption feature wavelengths. The appropriate methane absorption coefficients are very poorly known in this wavelength region, but we have made significant recent progress in understanding these absorption coefficients using the GEISA database. In this case, we can use the (now known) scatterer distribution to determine the absorbing gas distribution over the same vertical extent as the scatterers are known.

We also intend to mine the results for insight into the dynamics and general circulations of the planets. Latitudinal differences in tropospheric scatterer density as a function of altitude are indicative of vertical motions in the atmosphere. A good example of this is the elevated tropospheric cloud seen around Jupiter's equator. These clouds may be indicative of a Hadley cell type circulation occurring there<sup>3 xxx</sup>. If similar structures are identified on Neptune, the possibility exists of confirming or refuting hypothesized atmospheric circulations of these planets<sup>8</sup>. The latitudinal distribution of stratospheric scatterers on Neptune can be used to infer their source regions (polar magnetospheric effects, or solar-input controlled photochemistry), and the meridional spreading they experience compared to their fallout rates (indicated by their latitudinal homogeneity or lack thereof). As with the scatterer abundance, the vertical, latitudinal and longitudinal variations of methane abundance are also indicative of atmospheric motions and condensations. The general circulation should influence the tropospheric meridional-vertical cross section of methane mixing ratio. Finally, if we identify latitudinal and/or longitudinal differences in Neptune's stratospheric methane abundance, it may be indicative of convective penetration events thought to be responsible for the possible stratospheric methane mixing ratio enhancement over cold trap amounts on Neptune.

### **Acknowledgements**

Observations at the Palomar Observatory were made as part of a continuing collaborative agreement between Palomar Observatory, the Jet Propulsion Laboratory, and Cornell University. Partial support for this research has been provided by NASA Planetary Astronomy Program, NAG 5-7919.

### **References (following page)**

- 1 Hayward, T., Brandl, B., "Palomar High Angular Resolution Observer," in preparation.
- 2 Baines, K. H., and Bergstrahl, J. T., "The structure of the Uranian atmosphere: Constraints from the geometric albedo spectrum and H<sub>2</sub> and CH<sub>4</sub> line profiles," *Icarus*, **65**, 406–441, (1994).
- 3 Banfield, D., Conrath, B. J., Gierasch, P. J., Nicholson, P. D., Matthews, K., "Near-IR spectrophotometry of Jovian aerosols – meridional and vertical distributions," *Icarus*, **134**, 11–22, (1998).
- 4 Banfield, D., Gierasch, P. J., Squyres, S. W., Nicholson, P. D., Conrath, B. J., Matthews, K., "2 $\mu$ m spectrophotometry of Jovian stratospheric aerosols – scattering opacities, vertical distributions and wind speeds," *Icarus*, **121**, 389–410, (1996).
- 5 Borysow, A., "New model of collision-induced infrared-absorption spectra of H<sub>2</sub>–He pairs in the 2–2.5 $\mu$ m range at temperatures from 20 to 300K – an update," *Icarus*, **96**, 169–175, (1992).
- 6 Baines, K. H., Hammel, H. B., Rages, K. A., Romani, P. N., Samuelson, R. E., *Clouds and Hazes in the atmosphere of Neptune*, chapter in *Neptune and Triton*, D. P. Cruikshank, ed., U. Arizona Press, Tucson, (1995).
- 7 Baines, K., H., Hammel, H. B., "Clouds, hazes and the stratospheric methane abundance ratio in Neptune," *Icarus*, **109**, 20–39, (1994).
- 8 Conrath, B. J., Flasar, F. M., Gierasch, P. J., "Thermal structure and dynamics of Neptune's atmosphere from Voyager measurements," *J. Geophys. Res. Suppl.*, **96**, 18931–18939, (1991).